scientific reports

Check for updates

OPEN

Seawater temperature recorded in the last phase of Late Cretaceous in the Yarkand Basin

Yaping Li[1], Jun Wang[2], Sibo Yang[3] & Yangtong Cao[4]✉

The salt-bearing strata of the Tuyiluoke Formation, developed in the western Tarim Basin in the last phase of the Late Cretaceous, have sparse paleo-temperature records for this period. Given the high sensitivity of halite to temperature fluctuations in evaporative basins, the homogenization temperature of fluid inclusions in primary pure liquid-phase halite not only reflects the surface brine temperature of ancient salt lake during the crystallization process but also serves as an indicator of paleoclimate under evaporative conditions. The paper reveals that the homogenization temperature of primary pure liquid inclusions during the ancient salt lake's formation period ranges from 9.1 to 35.0 °C, with an average of 22.7 °C. This represents the brine or paleo-seawater temperature during this period and suggests that the brine or atmospheric temperature underwent two significant fluctuations. Overall, there is a cooling-warming-cooling trend (average homogenization temperatures transitioning from 23.3 to 16.7 °C, then to 23.9 °C/25.7 °C/26.7 °C, and finally to 15.5 °C), reflecting periodic changes in paleoenvironmental temperatures during the salt lake developmental phase. In other regions of the Tethys domain, it has been observed that the mean temperature during the Late Cretaceous-Early Eocene to middle Eocene initially increased and subsequently decreased (22.7 °C/23.8 °C → 27 °C/28°C → 31.8 °C/31°C → 25.6 °C), aligning with global paleoclimate and seawater temperature trends for the same period. The temperature data provide providing new evidence for the paleo-temperature of the northwestern part of the Tarim Basin during the Late Cretaceous period.

Keywords Seawater temperature, Halite fluid incluisons, Late cretaceous, Yarkand basin

The evaporites is typically closely associated with tectonic activities, transgression-regression cycles, closed basins, and arid climatic conditions[1–4]. During the Late Cretaceous to Paleogene period, the western Tarim Basin (also referred to as the Yarkand Basin) underwent multiple transgression-regression cycles[5–9]leading to the development of two distinct evaporites sequences: the Late Cretaceous Tuyiluoke Formation, primarily composed of sandstone, mudstone, silty mudstone, gypseous mudstone, thin gypsum rock, and lenticular rock salt, formed under a marine regressive settings during the Late Cretaceous; and the Aertashen Formation, mainly consisting of thick-massive gypsum and anhydrock layers interbedded with mudstone (sandstone) and limestone (argillaceous limestone), which developed in an intermittent marine transgressive sedimentary environment during the Paleocene (Fig. 1a). Over the past few decades, paleontological and mineralogical indicators have significantly advanced the reconstruction of paleotemperatures. However, there are limited reports on Late Cretaceous paleotemperature records from the Yarkand Basin in the eastern Tethys Region. The extremely thick evaporites deposited under arid conditions in this basin largely restrict the applicability of traditional climatic and environmental indicators, thereby impeding a comprehensive understanding of the Late Cretaceous paleotemperatures in the Yarkand Basin.

Due to the high sensitivity of rock salt to temperature fluctuations in evaporative basins, it plays a crucial role in paleoclimate reconstruction. This significance is demonstrated by the fact that during the formation process, rock salt crystals capture salt lake brines and form fluid inclusions. The homogenization temperatures of these fluid inclusions record detailed information about water and atmospheric temperatures at the time of their formation[10,11]. Previous studies have indicated that since halite forms in shallow brine environments during evaporation (typically no deeper than 2 m), the homogenization temperatures of fluid inclusions in primary pure liquid-phase halite not only reflect the surface brine temperature of ancient salt lakes during the crystallization process[12] but also approximate the temperature conditions under ancient evaporative

[1]Development and Research Center, China Geological Survey, Beijing 100037, China. [2]Institute of Geology, Chinese Academy of Geological Sciences, Beijing 100037, China. [3]School of Earth Sciences, East China University of Technology, Nanchang 330013, China. [4]MNR Key Laboratory of Metallogeny and Mineral Assessment, Institute of Mineral Resources, Chinese Academy of Geological Sciences, Beijing 100037, China. ✉email: cyt1941@126.com

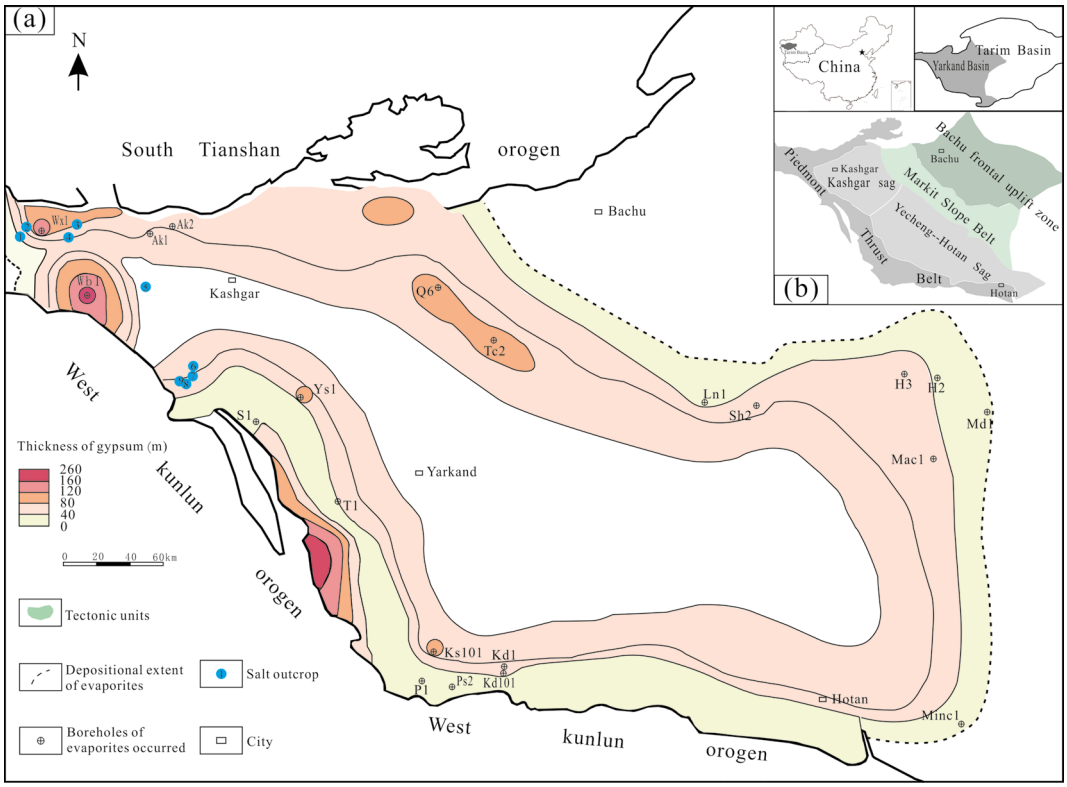

Fig. 1. Rock salt outcrop and isopach map of gypsum rock in Yarkand Basin (**a**) and its tectonic division (**b**).

environments[11,13]. Furthermore, given the strong correlation between water and air temperatures, which are representative paleoclimate indicators, the homogenization temperatures can serve as proxies for water or air temperatures at the time of formation[14–16].

However, research on evaporites in the Yarkand Basin has predominantly focused on salt-bearing strata, mineral assemblages, and geochemical characteristics[17,18]as well as the extent of Mesocenozoic transgressions[19–23] for many years, but no studies have been conducted on salt inclusions from the ancient salt lake in the basin. Consequently, the surface of brines or paleoclimate temperatures during the sedimentation process of the ancient salt lake remain unknown. Over the past decade, investigations into the temperature measurement of salt inclusions in ancient evaporative basins across China (e.g., the Lanping-Simao Basin in Yunnan Province, Sichuan Basin, Jiangling Depression in Hubei Province, Kuqa Depression in the northern Tarim Basin, etc.) have been carried out, with numerous relevant publications emerging. However, such studies have not yet been extended to the Yarkand Basin in the western Tarim Basin. In this study, halite cuttings from the Wb1 borehole, which are well-developed in the central part of the basin, were selected for salt inclusion temperature measurements. This aims to determine the surface temperature of brines during the halite sedimentation process and further reflect the temperature characteristics of the paleoenvironment during this period.

Geological background

The Yarkand Basin is located in the western Tarim Basin, as a foreland basin which developed from the Pre-Sinian basement has been reformed multiple times by tectonic superimpositions[24,25]. From the West Kunlun piedmont to the interior of the basin, it is characterized by a piedmont thrust belt, central sag, which divided the Kashgar and Yecheng-Hotan sags, the Markit slope belt, and the Bachu frontal uplift zone sequentially[26,27] (Fig. 1b). The Yarkand Basin was an inherited graben basin in the early Cretaceous, but during the late Cretaceous-Paleogene it had begun to develop into a foreland basin, with its depositional center distributed along the West Kunlun to South Tianshan piedmonts[20]. Since the Cenozoic era, the basin has subsided and deformed, developing several subsiding centers and very thick depositional cap rocks due to the collision of the Indian and Eurasian plates[28]. In the Neogene, the maximum depositional thickness of this basin was located in the Yecheng-Hotan sag, but its depositional center has already migrated along the northwest line to the Kashgar sag since the Quaternary[29].

In the early Cretaceous, the Yarkand Basin was a strip-shaped graben basin with NW-SE orientation located at the West Kunlun piedmont with a largest subsiding center[30]. Sedimentation into the basin was controlled by the provenances of the South Tianshan and West Kunlun orogens. Sediments were distributed along the long strip-shaped West Kunlun piedmont, with thickness gradually decreasing from SW to NE orientation, developing into an alluvial fan, fan delta, and shore-neritic sub-facies[31]. In the late Cretaceous, a braided river delta, supratidal evaporated sand-mud flat, and a carbonate platform developed sequentially[23] and a salt-gypsum flat was deposited in the basin. In the Paleocene-early Eocene, this basin developed into a semi-closed estuarine

and lagoon environment. Affected by terrigenous debris and subtropical dry climate[21,22]clastic rocks, in addition to evaporites and carbonates, were developed during this period. The main evaporative sequences are the Tuyiluoke and Aertashen Formations, but the former is smaller than the latter on the extent or scale.

Materials and methods

A total of 35 halite cuttings samples from well Wb1 (the Tuyiluoke Formation of Upper Cretaceous) were selected for thin section grinding (Fig. 2a), and temperature measurement of salt fluid inclusion was carried out. First select the crystal form of regular and pure halite, and thoroughly clean with anhydrous ethanol to ensure that its surface is clean and flawless. Then, the treated halite sample was cut along its cleavage plane with a knife to a 1–2 mm slice, and then microscopic petrographic observation was carried out to record the size, shape and distribution characteristics of the fluid inclusions in halite. The primary salt fluid inclusions were analyzed and selected, and the selected primary halite crystals were sealed with plastic self-sealing bags and stored in desiccant. The temperature measurement and analysis of fluid inclusions were carried out in the Ministry of Natural Resources Key Laboratory of Metallogeny and Mineral Assessment.

The fluid inclusions were observed under microscope and the pure liquid phase primary inclusions were selected. The single liquid phase inclusion sheet is placed under the microscope for overall observation and photography, focusing on recording the combination and morphology of the primary inclusion formed in the early diagenesis and the secondary inclusion formed by recrystallization, and the measured area is marked out. Then the inclusion sheet is cut into small pieces suitable for temperature measurement (generally about 1 cm × 1 cm), and the small inclusion sheet to be measured is placed on the hot and cold platform. Constant temperature freezing is carried out, and the general freezing temperature is − 18 ℃[32]. After bubbles appeared in freezing nucleation of a single liquid phase inclusion, the homogenization temperature test was carried out. The Linkam THMSG600 cold and hot platform was used to complete the homogenization temperature test, and the heating rate was 0.5 ℃/min. When the bubbles gradually became smaller, the temperature was temporarily reduced to 0.1 ℃/min. The homogenization temperature (T_h) test of fluid inclusion in rock salt is divided into two parts: single liquid inclusion and gas–liquid two-phase inclusion. The homogenization temperature of the primary single liquid phase inclusions can reflect the surface temperature of the brine during crystallization. The time of thermal event can be predicted by the homogenization temperature obtained from the test of gas-liquid

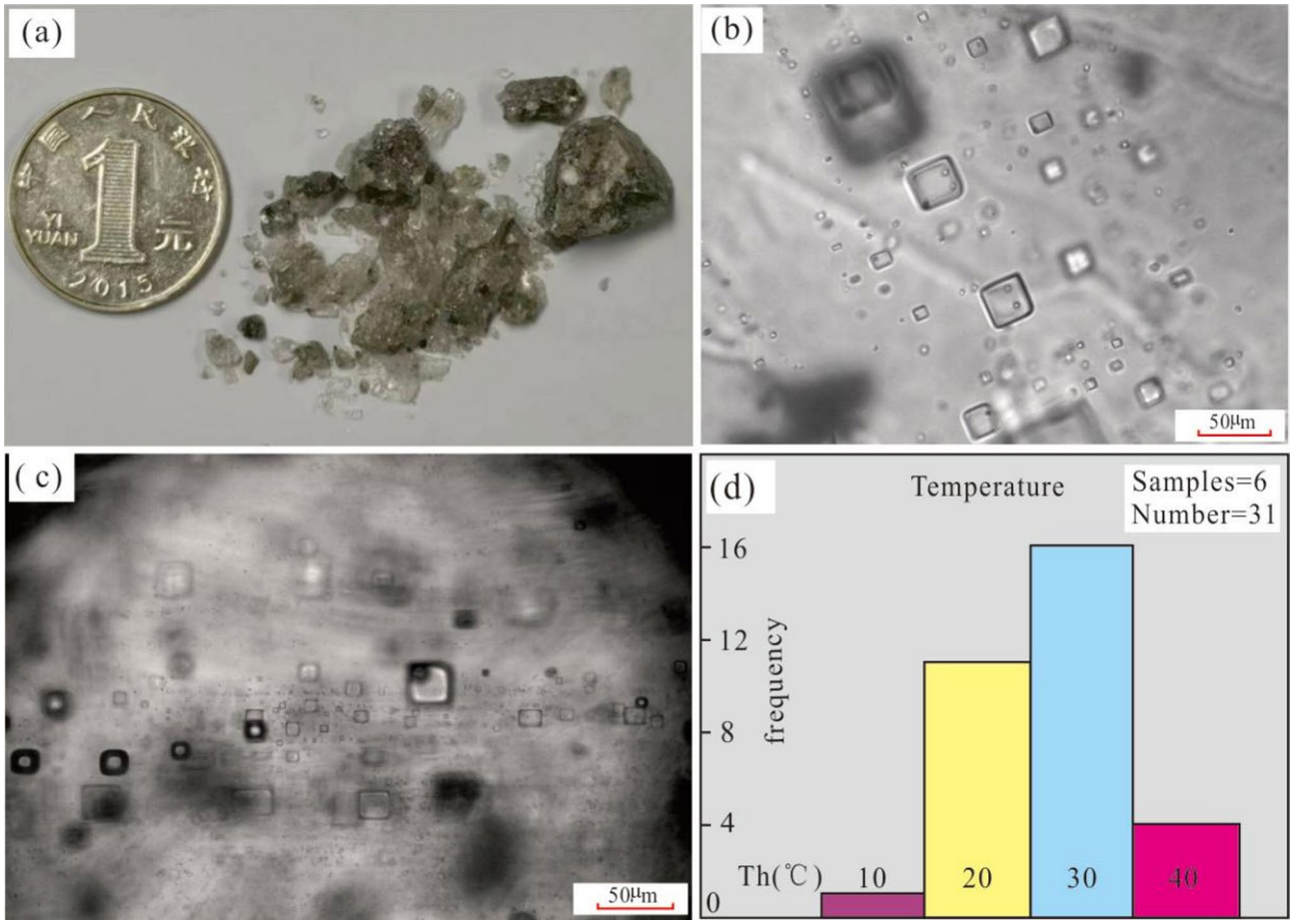

Fig. 2. Rock salt of well Wb1 from Tuyiluoke Formation (**a**), Primary fluid inclusions (**b**), secondary fluid inclusions (**c**), and histogram of the homogenization temperature with 6 samples and 31 data statistics (**d**).

two-phase inclusions. Because the repeated temperature-cooling test process may lead to certain errors in the results[13] in order to ensure the accuracy of the test results, only one temperature measurement experiment was conducted for all samples.

Results

Fluid inclusions are well developed in the halite of the Cretaceous Tuyiluoke Formation in well Wb1, the Yarkand Basin, and primary and secondary fluid inclusions are found under microscope. The fluid inclusions are single liquid and gas–liquid two phases. The gas-liquid ratio of the two-phase fluid inclusions is usually less than 5%, and the individual fluid inclusions can reach 8%. The primary fluid inclusions are mainly distributed in strips of light and dark, and individual fluid inclusions appear as negative crystals, square or rectangular, with sizes ranging from 2 to 70 μm (Fig. 2b,c). The secondary fluid inclusions are mostly irregular, without edges, and have large size changes, usually cutting through crystals, and most of them are gas-liquid two-phase, and the gas-liquid ratio changes greatly.

In this temperature measurement experiment, after screening 35 experimental samples, the pure liquid phase homogenization temperature of 31 data points of 6 samples was measured, among which the homogenization temperature of halite fluid inclusions of Wb1-6191.20 was between 9.1 ℃ and 20.3 ℃, with an average of 15.5 ℃. The homogenization temperature of halite fluid inclusions in Wb1-6193.25 was between 13.1 ℃ and 32.8 ℃, with an average of 25.0 ℃. The homogenization temperature of fluid inclusions in halite sample Wb1-6193.50 is 25.7 ℃. Similarly, in Wb1-6193.70 samples is 23.9 ℃, in Wb1-6194.35 sample was between 15.7 ℃ and 17.7 ℃, with an average of 16.7 ℃. The homogenization temperature of halite fluid inclusions of Wb1-6194.95 samples ranged from 13.5 ℃ to 35.0 ℃, with an average of 23.3 ℃ (Table 1). The minimum value of the overall homogenization temperature is 9.1 ℃, the maximum is 35 ℃, and the average is 22.7 ℃ (Table 1). The distribution trend of temperature data is shown in Fig. 2d.

Discussion

Rationality of data

Because the halite is easy to deliquesce and dissolve, it may easily change in the process of burial and preservation, which will affect the reliability and stability of Homogenization temperature (T_h) data, especially for the halite samples in ancient salt lakes[11]. However, when the halite crystal precipitates in a shallow water environment, the temperature captured by the fluid inclusion is approximately T_h, without pressure correction, and can directly reflect the temperature condition when the rock salt is deposited[11]. In this study, we rigorously verify whether the primary fluid inclusions are altered or destroyed by thermal rebalancing through two approaches. On the one hand, the consistency of T_h data in a given fluid inclusion assemblage is analyzed. Goldstein and Reynolds[33] pointed out that if the fluctuation range of about 90% T_h data within a single fluid inclusion assemblage is less than 15 ℃, it can indicate that the primary fluid inclusions are not affected by obvious thermal rebalancing. The results of this paper conform to this standard (Table 1). The temperature range of all T_h data of fluid inclusion assemblage samples measured is less than 15 ℃, with the minimum value of 2 ℃ and the maximum value of 13.2 ℃, which strongly proves that the rock salt crystal remains relatively stable in terms of thermal rebalancing and does not cause significant interference to T_h data.

In addition, large halite inclusions are theoretically more malleable than small halite inclusions, and their T_h value will be higher than the actual trapping temperature if stretched[34–36]. But the results of this study show that: There is no obvious correlation between the size of fluid inclusions and the corresponding T_h (Fig. 3), which further supports the conclusion that thermal rebalancing has not caused substantial changes or damage to the halite crystals and T_h data, and fully indicates that the T_h data obtained by us can more accurately reflect the surface temperature and atmospheric temperature of the ancient salt lake brine during the Late Cretaceous Tuyiluoke Formation development.

Temperature characteristics

Based on the mean and maximum homogenization temperature data of halite at different locations in the drilling profile (Fig. 4), the variation characteristics of brine temperature are preliminarily inferred. The results show that the brine temperature or atmospheric temperature has experienced a great fluctuation from the bottom of the drilling profile to the top, showing a cooling–warming–cooling trend on the whole (average homogenization

Samples	Size (μm)/T_h (℃)	T_{hAVG} (℃)		T_{hRANGE} (℃)
Wb1-6191.20	2×8/9.1; 3×3/17.1; 2×4/20.3	15.5		11.2
Wb1-6193.25	10×20/19.6; 3×3/19.8; 3×5/26.1; 3×3/27.5; 3×3/30.6;4×4/30.6; 4×4/32.8	26.7		13.2
Wb1-6193.50	5×5/25.7			
Wb1-6193.70	5×10/23.9		22.7	
Wb1-6194.35	4×12/15.7; 2×6/17.7	16.7		2.0
Wb1-6194.95	3×3/13.5; 4×3/16.7; 2×2/17.3; 4×4/16.7; 5×5/19.8; 4×4/22.7; 4×4/21.8; 20×5/26.3	23.3		12.8
	3×3/25.5; 3×3/25; 3×3/26.2; 6×6/26.7; 4×4/25.7; 4×4/26.5; 10×3/29.4; 3×5/35.0			10.0

Table 1. Homogenization temperatures of cumulate fluid inclusions of the Tuyiluoke formation in Yarkand Basin. T_{hAVG} average homogenization temperature, T_{hRANGE} range of the *T*h data, *FIA* fluid inclusion assemblage.

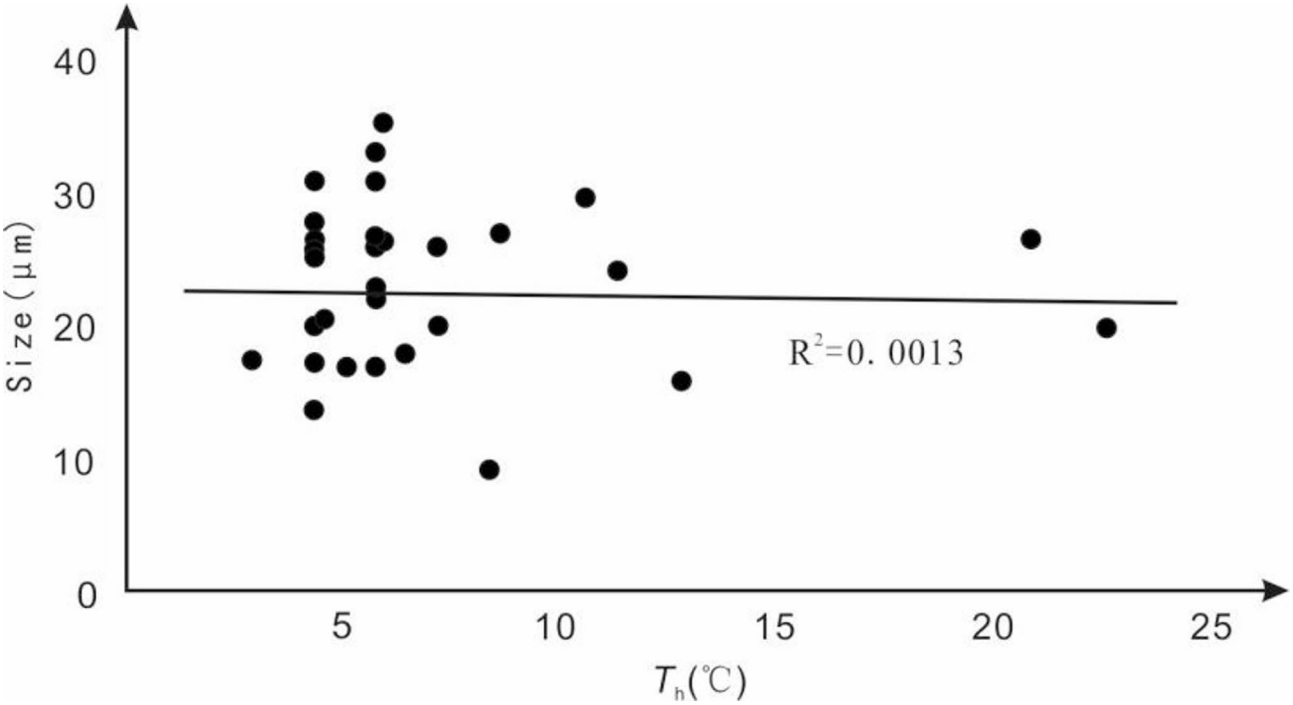

Fig. 3. Cross-plot of the T_h data plotted against size of fluid inclusions.

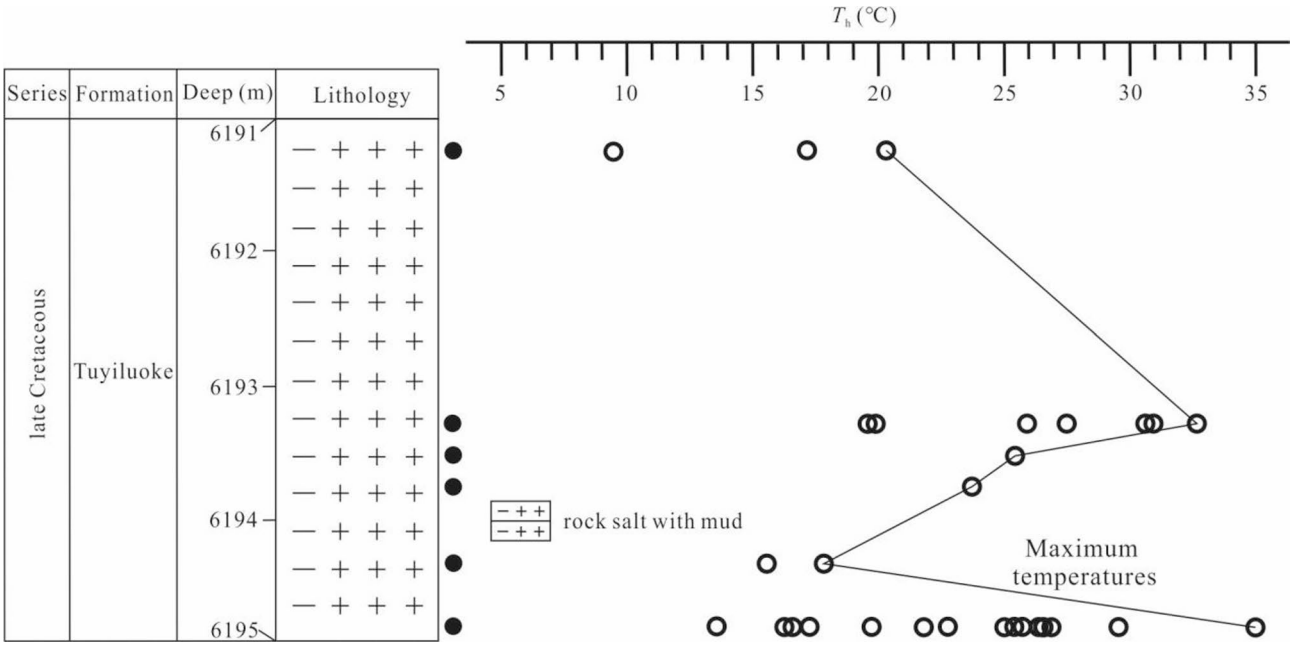

Fig. 4. Temperature change trend indicated by T_h from core Wb1.

temperature ranging from 23.3 ℃–16.7 ℃–23.9 ℃/25.7 ℃/26.7℃–15.5 ℃). There are two cycles of temperature change from high to low. The average temperature of the sample 6194.95 m at the bottom of the profile is 23.3 ℃, which represents the average temperature of the paleo-lake surface during this period (halite deposited period), but the maximum value of 35.0 ℃ may record the highest atmospheric temperature and paleo-brine temperature during this period. The average and maximum temperature of samples 6194.35 m were 16.7 ℃ and 17.7 ℃ respectively, showing a rapid downward trend. In contrast, temperature warming is revealed in the upper part (sample 6193.70 m, 6193.50 m and 6193.25 m), the average homogenization temperature rose to 26.7 ℃, and finally dropped to 15.5 ℃ in sample 6191.20 m, which reflects the periodic change of paleoenvironmental temperature during the salt lake developmental period. Due to the small thickness of the salt section (3.75 m

in total), the temperature change will not be too long on the time scale, and can only reflect the change of the surface temperature of the brine in the ancient salt lake during the halite depositional period.

Comparison of ancient seawater temperature in Tethys domain

The comparison of the paleotemperature reflected by the fluid inclusions of halite with other regions of the world at the same time can provide a key clue for understanding the regional geological evolution and paleoclimate pattern. The average temperature of halite fluid inclusion in Mengyejing potash deposit in Yunnan Province, which is also a Late Cretaceous Tethys seawater deposit, is 23.8 ℃[37]which is similar to the average temperature value in this study. In addition, according to the study of Marine oyster fossils, the average temperature of paleo-seawater surface in the Eocene of Yarkand Basin is 27–28 ℃[38]. From the salt-forming belt, the evaporative series in Yarkand Basin mainly developed in the late Cretace-Paleocene, and the Kuqa Basin in the east of the basin, which has the same salt-forming material source, and later salt-forming age, Paleocene-Eocene. Xu Yang et al.[15,16] recovered an average temperature of 31.8 ℃ from the early Eocene halite fluid inclusion in Kuqa Basin, and the homogenization temperature of the Middle Eocene halite fluid inclusion showed that the average temperature was 25.6 ℃. Early Eocene Marine mollusc assemblage in the Paris Basin of the Tethys Domain, was studied with high precision, with an average temperature of 31 ℃[39]. The Late Cretaceous-Early Eocene-Middle Eocene as a whole showed a process of first increasing and then decreasing, which is consistent with the global trend of paleoclimate and sea water temperature changes in the same period[40].

Conclusions

In this study, the homogenization temperature data of primary fluid inclusions in the Upper Cretaceous Tuyiluoke Formation in Yarkand Basin can provide quantitative evidence of paleo-seawater temperature. The homogenization temperature ranges from 9.1 to 35.0 ℃, with an average of 22.7 ℃, which represents the brine temperature or the paleo-seawater temperature of the halite depositional period. From the bottom up, the brine surface or atmospheric temperature of the ancient salt lake experienced two periodic fluctuation cycles from high to low, and the maximum temperature difference of the average temperature was 10.2 ℃. Considering the small thickness of halite profile, the paleoenvironment will not be too long on the time scale. This temperature difference reflects the temperature change of ancient brine at that time, and is basically consistent with the temperature change range of the Cretaceous-Paleogene geological history interface period. During the Late Cretaceous-Early Eocene-Middle Eocene, along with the gradual intrusion of seawater from the northwest margin of the Tarim Basin, the data of halite fluid inclusions show that the paleo-seawater temperature as a whole increased first and then decreased, which is consistent with the global paleoclimate and seawater temperature change trend in the same period. These values provide new evidence for the ancient seawater temperature or paleoenvironment temperature recorded of the northwestern Tarim Basin during the late Cretaceous period.

Data availability

All data generated or analysed during this study are included in this published article.

Received: 8 April 2025; Accepted: 9 June 2025
Published online: 03 July 2025

References

1. Yuan, J. Q., Huo, C. Y. & Cai, K. Q. The high Mountain-Deep basin saline environment: A new genetic model of salt deposits. *Geol. Rev.* **29**, 159–165 (1983).
2. Yuan, J. Q. *Proceedings of Salt Mine Geology of Professor Jianqi Yuan*, 1–104 (Xueyuan Press, 1989).
3. Qian, Z. Q., Wang, M. L. & Liu, C. L. *Continental Evaporites in China*, 34–86 (Geol. Publishing House, 1994).
4. Liu, C. L., Wang, M. L. & Jiao, P. C. Mesozoic-Cenozoic continental salt lake deposits and Potassium-Forming regularities in Northern China. *Acta Geol. Sinica*. **82**, 1725–1737 (2008).
5. Burtman, V. S. Cenozoic crustal shortening between the Pamir and Tien Shan and a reconstruction of the Pamir–Tien Shan transition zone for the retaceous and palaeogene. *Tectonophysics*. **319**, 69–92 (2000).
6. Bosboom, R. E. et al. Linking Tarim basin sea retreat (west China) and Asian aridification in the late eocene. *Basin Res.* **26**, 621–640 (2014).
7. Bosboom, R. E. et al. Late eocene sea retreat from the Tarim basin (west China) and concomitant Asian paleoenvironmental change. *Palaeogeogr. Palaeoclimatol. Palaeoecol.* **299**, 385–398 (2011).
8. Cao, Y. T. et al. Evaporite deposition and potassium enrichment prospect from upper cretaceous to paleogene in Yarkand basin, Xinjiang. *Mineral. Deposits*. **35**, 300–314 (2016).
9. Cao, Y. T. & Xu, H. M. A rapid Cu enrichment mechanism from Cu-bearing brine in Kuqa Basin, Xinjiang, China: Controlled by Crystallized Sequence of Saline Minerals. *Geofluids*. **2021**, 5550271 (2021).
10. Lowenstein, T. K., Jiarun, L. & Celeste, B. B. Paleotemperatures from fluid inclusions in halite: method verification and application to pleistocene evaporites, death valley, CA. *Chem. Geol.* **146**, 21–31 (1998).
11. Benison, K. C. & Robert, H. G. Permian paleoclimate data from fluid inclusions in halite. *Chem. Geol.* **154**, 113–132 (1999).
12. Zambito, J. J. & Kathleen, C. B. Extremely high temperatures and paleoclimate trends recorded in permian ephemeral lake halite. *Geology* **41**, 587–590 (2013).
13. Meng, F. W. et al. Homogenization temperature of fluid inclusions in laboratory grown halite and its implication for paleotemperature reconstruction. *Acta Petrologica Sinica*. **27**, 1543–1547 (2011).
14. Zhao, Y. J. et al. Late eocene to early oligocene quantitative paleotemperature record: evidence from continental halite fluid inclusions. *Sci. Rep.* **4**, 1–6 (2014).
15. Xu, Y., Cao, Y. T. & Liu, C. L. Brine temperature of early eocene salt formation period in Kuqa basin and its significance. *Earth Sci.* **46**, 4188–4196 (2021a).
16. Xu, Y., Cao, Y. T. & Liu, C. L. Mid-Eocene sea surface cooling in the Easternmost Proto-Paratethys sea: constraints from quantitative temperatures in halite fluid inclusions. *Int. J. Earth Sci.* **110**, 1713–1727 (2021b).
17. Chen, R. L. Geological characteristics of the tertiary Salt-Bearing sequences in Tarim basin. *Geol. Chem. Minerals*. **18**, 276–283 (1996).

18. Tan, H. B., Ma, H. Z. & Xiao, Y. K. Analysis on potash prospecting and distribution characteristic of Cl isotope in solid halite in Western Tarim basin. *Sci. China Ser. D Earth Sci.* **48**, 235–240 (2005).
19. Yong, T. S. & Shan, J. B. The development and formation in the Tarim basin in Cretaceous-P the development paleogene ages. *Acta Sedimentol. Sin.* **4**, 67–75 (1986).
20. Wang, Y. & Fu, D. R. The sedimentary-tectonic evolution of the Southwest Tarim basin from cretaceous to paleogene. *Acta Geol. Sinica*. **17**, 32–40 (1996).
21. Ma, H. D. & Yang, Z. J. Evolution of the cenozoic in Southwestern Tarim basin. *Xinjiang Geol.* **21**, 92–95 (2003).
22. Shao, L. Y. et al. A basin-Wide sequences stratigraphic analysis of the paleogene in Tarim basin. *J. Palaeogeography*. **9**, 283–292 (2007).
23. Zhuang, H. H., Guo, F. & Zhou, X. Evolution of sedimentary environment in late cretaceous, Kunlun mountain front, Tarim basin. *J. Xi'an Univ. Sci. Technol.* **33**, 39–45 (2013).
24. Hu, W. S., Chen, Y. S., Xiao, A. C., Liu, X. F. & Liu, S. G. Tectonic evolution and petroleum-bearing system in Southwestern Tarim basin. *Petrol. Explor. Dev.* **24**, 14–17 (1997).
25. Zhang, Y. B. Uplift of Tibet plateau and formation and evolution of the Southwestern intarim basin. *Xinjiang Petroleum Geol.* **20**, 6–10 (1999).
26. Zhang, D., Hu, J., Meng, Y., Zheng, M. & Fu, M. Characteristics of Qimugen thrust nappe structure in the Southwestern Tarim basin xinjiang, china, and its relationship with hydrocarbon. *Geol. Bull. China*. **26**, 266–274 (2007).
27. Fang, A., Ma, J., Wang, S., Zhao, Y. & Hu, J. Sedimentary tectonic evolution of the Southwestern of Tarim basin and West Kunlun orogen since late paleozoic. *Acta Petrologica Sinica*. **25**, 3396–3406 (2009).
28. Qu, G. S., Li, Y. & Li, Y. Structural segmentation and its factor in the Southwestern Tarim basin. *Sci. China Ser. D*. **35**, 193–202 (2005).
29. Ding, D. G. & Luo, Y. M. Collision structures in Pamir region and reformation of Tarim basin. *Oil Gas Geol.* **26**, 57–63 (2005).
30. Sun, L. D. Sedimentary facies and exploration of petroleum of the early cretaceous in Kuqa depression and Southwest depression in Tarim basin. *J. Palaeogeography*. **6**, 252–260 (2004).
31. Jia, J. H. Sedimentary characteristics and palaeogeography of the early cretaceous in Tarim basin. *J. Palaeogeography*. **11**, 167–176 (2009).
32. Zhao, Y. J. et al. Analytical method and paleoenvironmental interpretation of fluid inclusion homogenization temperature of ancient halite. *Acta Geoscientica Sinica*. **34**, 603–609 (2013).
33. Goldstein, R. H. & Reynold, T. J. Systematics of fluid inclusions in diagenetic minerals. *Soc. Sediment. Geol.* **31** (1994).
34. Petrichenko, O. I. Methods of study of inclusions in minerals in saline deposits. *Fluid Inclusion Res.* **12**, 114–274 (1979).
35. Roedder, E. & Howard, E. B. Thermal gradient migration of fluid inclusions in single crystals of salt from the waste isolation pilot plant site (WIPP). In *Scientific Basis for Nuclear Waste Management* (ed. Northrup, C. J. M.) 453–464 (Springer, 1980).
36. Roedder, E. The fluids in salt. *Am. Mineral.* **69**, 413–439 (1984).
37. Dong, J. et al. The characteristics of halite inclusions in the Mengyejing potash deposit Yunnan province, and their palaeoenvironmental fignificance. *Acta Petrologica Et Mineral.* **34**, 227–236 (2015).
38. Bougeois, L., Rafelis, M., Reichart, G. J., Nooijer, L. J., Nicollin, F. & Dupont-Nivet, G. A highresolution study of trace elements and stable isotopes in oyster shells to estimate central Asian middle eocene seasonality. *Chem. Geol.* **363**, 200–212 (2014).
39. Huyghe, D., Lartaud, F., Emmanuel, L., Merle, D. & Renard, M. Palaeogene climate evolution in the Paris basin from oxygen stable isotope ($\delta^{18}O$) compositions of marine molluscs. *J. Geol. Soc.* **172**, 576–587 (2015).
40. Song, H. J. et al. Seawater temperature and dissolved oxygen over the past 500 million years. *J. Earth Sci.* **30**, 236–243 (2019).

Acknowledgements

This work was supported by Deep Earth National Science and Technology Major Project (No. 2024ZD1003300) and Dissemination on Scientific and Technological Achievements of Geological Survey and Construction on Knowledge Service System (No. DD202510014).

Author contributions

Y.L. and Y.C. designed the study, completed the analysis and wrote the manuscript. J.W. and S.Y. conducted the experiments. All authors have read and agreed to the published version of the manuscript.

Declarations

Competing interests

The authors declare no competing interests.

Additional information

Correspondence and requests for materials should be addressed to Y.C.

Reprints and permissions information is available at www.nature.com/reprints.

Publisher's note Springer Nature remains neutral with regard to jurisdictional claims in published maps and institutional affiliations.